

An Improved Approach to Better Understand Power Electronics Variables*

A. NDTOUNGOU, AB. HAMADI and K. AL-HADDAD

Canada Research Chair in Energy Conversion and Power Electronics CRC-ECPE, École de Technologie Supérieure,
1100 Notre-Dame West Street, Montreal, Quebec H3C 1K3, Canada.

E-mails: augndtougou@yahoo.fr; abdelhamidhamadi@yahoo.fr, kamal@ele.etsmtl.ca

This paper aims to improve the teaching methodology for self-learning for teachers and students working in the area of power electronics. Three different methods have been proposed, mainly using mathematical equations, MATLAB/Simulink and MATLAB functions. This paper also proposes an easy way of calculating the exact values of the extinction angle known as ‘beta’. This avoids the use of the monogram known as the ‘Puchlowsky monogram’. In this paper the exact calculation of the rms load current for a single-phase controlled rectifier with R–L load is given. A three-phase controlled rectifier with a highly inductive load is also discussed in this paper with an interactive variable load resistance and inductance. The simulation results have been presented and extensive simulation and experimental studies have been carried out to analyze different waveforms under varying load conditions.

Keywords: education; power electronics; MATLAB; extinction angle; integration limits

1. Introduction

Power electronics is an important part of the electrical engineering curriculum as more than 75% of all generated power needs to be processed by power electronics converters [1–4]. The increasing demand for power quality, for speed control of ac motors, for smaller sized and lighter weight power supplies, and the expanding market demand for power electronic systems have made power electronics the fastest growing area in electrical engineering. Moreover, with increasing expansion of power electronics applications into commercial, industrial and residential sectors [5, 6], there is a demand for more sophisticated power electronics systems generating low harmonics to satisfy the needs of consumers. Therefore, it is necessary to have a better understanding of the impact of these recent technologies on the environment and a recognition of the urgent need for increased energy conservation. Consequently, it is necessary for learners, including students, to use all the tools available for the study and better understanding of power electronics circuits [7–9]. Thus, an effective power electronics course [10, 11] should ideally contain hands-on design and experimental work [12] in addition to the theoretical study, programming and simulation [9, 13]. Unfortunately, not many universities offer students the necessary tools to take advantage of the advances made and to study complex power electronic systems as needed by industry [14, 15]. At institution level, there is lack of effective curricula and necessary facilities for laboratory implementation. This paper is motivated primarily by the work currently underway at the ETS Engineering School of High Technology in Quebec (both at undergraduate and graduate levels). The authors believe that such content will help students and teachers in power electronics education and will help young faculty who are interested in pursuing academic careers, to get started in introducing power electronics courses. Brief proposals to improve teaching and also to show future trends in the field of power electronics will be presented with the help of a well planned questionnaire completed by the students. An investigation was undertaken to understand for their difficulties better and to offer suggestions for improvements in teaching methodology. From this work, we will try to provide answers to all these questions. In this paper, a different way of calculating the input and the output variables of a system in power electronics is proposed. This calculation may be made using the three proposed methods: (1) circuit simulation software to increase the students’ comprehension and calculation, (2) programming for the calculation and (3) theoretical calculation. Finally, an interesting method is also provided for simulation studies under varying conditions of varying parameters.

2. Investigation

2.1 Theory

The remarks and recommendations of the students include the following.

- The handbooks of course, practical work and directed work must be available before the beginning of the session.
- The theory given in the course should be well organized.
- There was a problem with checking the results of specified problems.
- There was a problem with reading the nomograms for the calculation of the extinction angle β and the rms load current.
- There was real time variation of system parameters.

2.2 Simulation

A common complaint is that special programming and simulation tools are unavailable and not offered to the students. These tools must be available to them.

2.3 Experimentation

Additional meetings for laboratory experiments should be offered in order to familiarize the students with the available materials and to understand their operation.

3. Solution proposed

3.1 Theory and simulation

No change in the contents of the power electronics notes should be made during the session in order to avoid destabilizing the students. Additional meetings of the MATLAB courses should be offered at the beginning of the course; these will help the students to gain a better understanding and to have an autodidactic (self-learning) approach.

The goal of these meetings of MATLAB, is to allow the students:

1. to familiarize with the MATLAB/Simulink environment,
2. to correct themselves with simulations and programming,
3. to learn continuous and discrete simulation,
4. to learn security issues,
5. to perform fault analysis.

Most universities do not provide separate courses on Power Electronics modeling and simulation programs. One- or two-week short courses may be provided to allow the students to familiarize themselves with simulation and programming, which cannot be linked to the regular curriculum. The contents are usually on simulation tool manuals such as MATLAB/Simulink, Pspice, PSIM [16].

Familiarity with software sections, MATLAB, Labview and Simplis, is strongly recommended before enrolling on the regular Power Electronics courses.

3.2 Experimentation

The experimental part of the course is crucial in Power Electronics education. However, most universities do not possess well-equipped experimental laboratories for Power Electronics; only the basics, to do some simple experiments, are provided. There must be more emphasis on the importance of using simulation software in Power Electronics education. Using simulation software will help students to better understand the theory and to complement their lack of experimental experiences in hardware/software. In particular, use of simulation software will help young aspiring students to understand better the complexities of a circuit, particularly when they are more comfortable with using a computer than learning through mathematics. It also helps most students to work out the basic operation of power electronics circuits. They can design and analyze the complex power electronics circuits easily using simulation, thereby expecting better results.

4. Rectifiers

4.1 Single-phase controlled rectifier

4.1.1 Calculation of beta

As an example, we chose a simple power electronic circuit, called a single-phase controlled rectifier, which is studied in the first chapter of a power electronic course. In this circuit, calculation of the extinction angle for a given firing angle is important and can only be obtained by solving a non-linear equation. The goal here is to show how to determine the extinction angle, β , by two methods: the first method uses a nomogram,

which gives the approximate value and the second method uses the MATLAB function 'fsolve', which gives a more precise value. The rms value of the load current, I_{LR} , will then be calculated by three methods using the nomogram and the normalized current I_{NRL} versus the firing angle, α , for a load angle given, ϕ . The first method of calculating this rms current uses a MATLAB integral function; the second one uses a simulation study of the circuit and, finally, the third uses the theoretical calculation. We will conclude that the results of the three methods give about the same value for the rms value of load current.

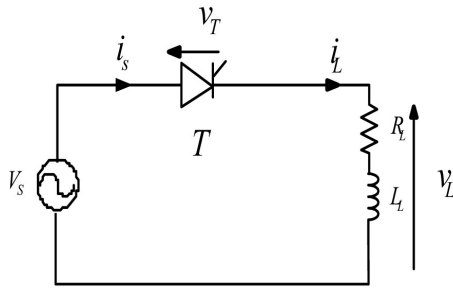


Fig. 1. Single-phase controlled rectifier.

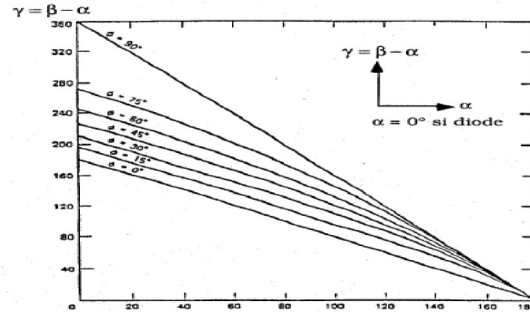


Fig. 2. Duration of conduction $\gamma = f(\alpha)$ for different ϕ .

Exact expression of the load current i_L

The circuit in Fig. 1 is described by the differential equation

$$v_s(t) = V_{\max} \sin \omega t = L_L \frac{di_L}{dt} + R_L i_L \quad (1)$$

z_L : load impedance, $z_L = \sqrt{R_L^2 + (L_L \omega)^2}$; R_L : load resistance, L_L : load inductance,

$$i_L = \begin{cases} \left(\frac{V_{\max}}{Z_L} \right) \cdot \left[\sin(\omega t - \phi) - \sin(\alpha - \phi) e^{-\left(\frac{t-\alpha}{\tau}\right)} \right] & \text{for } \alpha < \omega t < \beta \\ 0 & \text{for } \beta < \omega t < 2\pi \end{cases} \quad (2)$$

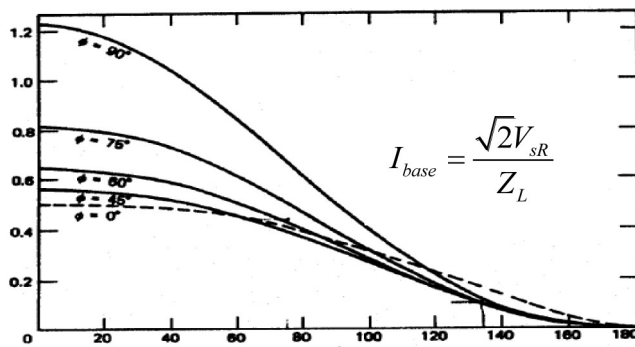


Fig. 3. Normalized current I_{NLR} versus firing angle α for different load angles ϕ .

Phase voltage and frequency	$V_{sR} = 120V, f_s = 60Hz$
Source voltage type of nonlinear load	$L_L = 40mH, R_L = 15\Omega$
Load angle	$\phi = 45^\circ$
Firing angle	$\alpha = 30^\circ$

Table 1. Specification parameters.

To find β , one should solve the following equation:

$$\sin(\beta - \phi) - \sin(\alpha - \phi) e^{-\frac{\beta - \alpha}{\tau}} e^{\frac{\alpha}{\omega\tau}} = 0 \quad (3)$$

The two methods to determine the extinction angle β are as follows.

(a) 1st method by the nomogram

This method used in the power electronics course uses a nomogram, called the Puchlowsky nomogram, which gives the variation of the conduction angle γ versus firing angle α for a given ϕ . The extinction angle β is given by the relation:

$$\gamma = \beta - \alpha. \quad \phi = \arctg\left(\frac{\omega L_L}{R_L}\right) = 45^\circ, \quad \text{however } \gamma = \beta - \alpha \Rightarrow \beta = \gamma + \alpha = 196 + 30 = 266^\circ.$$

(b) 2nd method (MATLAB function 'fsolve')

This uses a MATLAB function 'fsolve', which solves the nonlinear systems of equations. The initial condition is chosen for $x = 3.5$ and the optimization will run until an error tolerance of $1e^{-6}$ is met. The calculated value of β is given in the last line of the program.

```
function F = fx2(x);
LL = 0.04; RL = 15 ; W = 377; A = pi/6; PHI = atan(LL*W/RL); taux = LL/RL;
F = sin(x(1)-PHI)-sin(A-PHI).*exp(-x(1)/(W*taux)).* exp(A/(W*taux));
End (To erase)
```

To calculate β , one uses

```
clc
x=3.5;
options = optimset('Display','off','ToIX',1e-6);
x = fsolve('fx2',x,options);
fprintf(1,'RESULTS: The extinction angle is \n');
fprintf(1,'x = %8.4f \n',180*x/pi);
```

One finds: $\beta = 225.65^\circ$. From the method suggested, one plots several curves of $\beta = f(a)$.

4.1.2 Calculation of the rms current

The value of the rms current is not easy to find analytically and the calculation is done in three different ways: using the nomogram, programming the MATLAB integral function and, finally, by numerical simulation of the studied circuit.

(a) 1st method

This method uses the Puchlowsky nomogram that, starting from the standardized current, makes it possible to determine the rms value of the load current.

This normalized current is given by the following formula:

$$I_{NRL} = \frac{I_{LR}}{I_B} \quad (4)$$

With I_B : Basic current;

$$I_B = I_{base} = \frac{V_{max}}{Z_L} = \frac{\sqrt{2}V_{SR}}{Z_L} = 7.98A \quad (5)$$

From the nomogram: $\phi = 45^\circ$, $\alpha = 30^\circ$, $I_{NRL} = 0.55$ (6)

The rms load current is therefore: $I_{LR} = I_B * I_{NRL} = 4.38A$ (7)

(b) 2nd method

The method uses programming of the MATLAB integral function. The function is the integral of the square of the rms value of the current. The last part of the programming gives the square root of the function with its integration limits expressed in radians.

```
function y = f(x);
LL = 40e-3; RL=15; w=2*pi*60; ZL= sqrt(RL^2+(LL*w)^2); Vmax = 120*sqrt(2);
phi = atan(LL*w/RL) ; alpha = 30*pi/180; taux = LL/RL; A = exp(alpha/(w*taux));
y = (Vmax/ZL)^2*(1/(2*pi)).*(sin(x-phi)- sin(alpha -phi).*exp(-x/(w*taux))*A).^2;
```

To calculate the integral, one uses

```
a1 =sqrt(quad( 'f' , 30*pi/180 , 225.65*pi/180))
```

One finds $I_{LR} = 4.28 A$

One then generalizes this result by tracing the rms load current I_{LR} versus the firing angle α for various values of the load.

(c) 3rd method (by simulation)

One uses the block in 'SimPowerSystems' of MATLAB. In the circuit, one puts the voltage drop of the thyristor at near zero for a better comparison with the theoretical values. To read the rms value, one chooses RMS Discrete block for the calculation of the rms value of the load current I_{LR} . Therefore $I_{LR} = 4.28 A$.

We can thus affirm that the two other methods suggested give similar results to those obtained by simulation. It is thus more reliable than the method used at present using the nomograms.

4.2 Controlled single-phase full-wave rectifier

In this example (Fig. 4; Table 2), one seeks to determine the rms load current I_{LR} in discontinuous conduction mode for $\alpha = 60^\circ$. Initially, one determines the extinction angle β , first by using the Puchlowsky nomogram, by using the method suggested using the MATLAB function 'fsolve', of these two methods, the proposed method is the more precise. Then, we use the three proposed methods to calculate the rms value of the load current; the first uses the theoretical calculation, the second is the simulation and the third uses the MATLAB function integral.

In continuous conduction mode, the integration limits to determine the rms value of the load current I_{LR} vary from α to $\pi + \alpha$. One can also determine the rms value of the load current using Fourier analysis and the simulation.

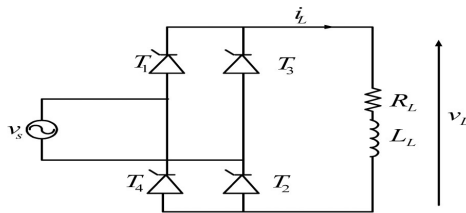


Fig. 4. Controlled single-phase full-wave rectifier.

Phase voltage, and frequency	$V_{sR} = 120V, f_s = 60Hz$
Voltage-source type of nonlinear load (discontinuous mode)	$L_L = 40mH, R_L = 15\Omega$ $\alpha = 60^\circ$
Voltage-source type of nonlinear load (continuous mode)	$L_L = 40mH, R_L = 15\Omega$ $\alpha = 20^\circ$

Table 2. Specification parameters.

(a) Simulation results

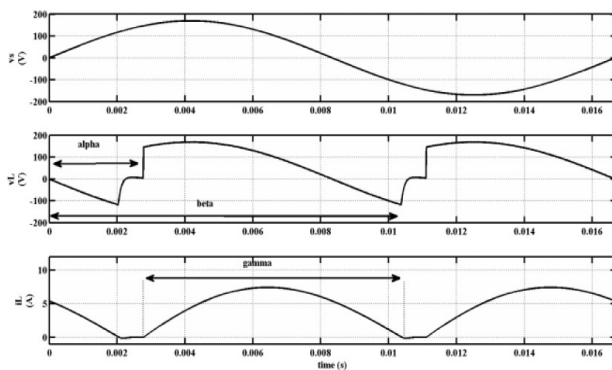


Fig. 5. Discontinuous mode $v_s(V), v_L(V)$ and $i_L(A)$.

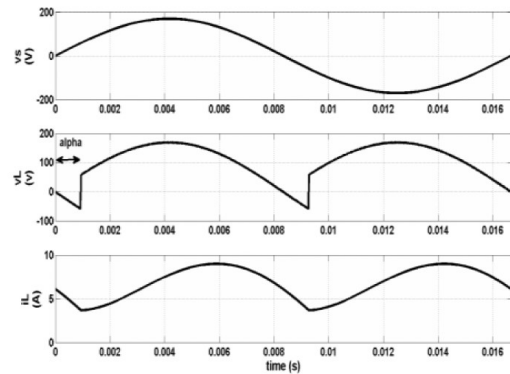


Fig. 6. Continuous mode $v_s(V), v_L(V)$ and $i_L(A)$.

(b) Experimental results

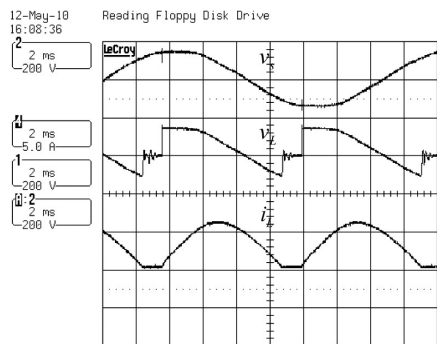


Fig. 7. Discontinuous mode $v_s(V), v_L(V)$ and $i_L(A)$.

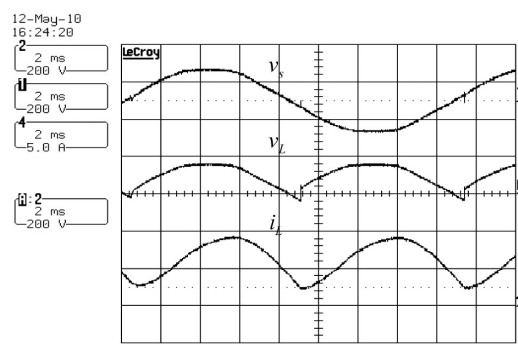


Fig. 8. Continuous mode $v_s(V), v_L(V)$ and $i_L(A)$.

4.2.1 Calculation of beta

4.2.1.1 Discontinuous mode: $\alpha = 60^\circ$ and $\phi = \arctan\left(\frac{\omega L_L}{R_L}\right) = 45^\circ$

	By the nomogram	By using the MATLAB function 'fsolve'
Calculation of β	$\beta = \gamma + \alpha = 170^\circ + 60^\circ = 230^\circ$	$\beta = 224.3^\circ$

	By theoretical calculation	by using the MATLAB function integral
Calculation of the rms load current with $\beta = 224.3^\circ$	$I_{LR} = \sqrt{\frac{1}{\pi} \int_0^\beta \left(\frac{V_{max} \sin \omega t}{Z_L}\right)^2 d\omega t} = 5.33A$	$I_{LR} = 5.07 A$

4.2.1.2 Continuous mode: $a = 20^\circ$

Calculation of the rms load current

The Fourier analysis is given by

$$v_L = V_L + \sum_{n=1}^{\infty} a_n \cos n\omega t + \sum_{n=1}^{\infty} b_n \sin n\omega t \tag{8}$$

The controlled full-wave bridge rectifier parameters are given below:

$$V_{sR} = 120V, \quad F = 60Hz, \quad R_L = 15\Omega, \quad L_L = 40mH, \quad \alpha = 20^\circ$$

	Expression	
Average load current and load voltage	$I_L = \frac{V_L}{R_L}$ and $V_L = \frac{2V_{max}}{\pi} \cos \alpha$	
Fourier components calculation	$a_n = \left(\frac{2V_{max}}{\pi}\right) \left[\frac{\cos(n+1)\alpha}{(n+1)} - \frac{\cos(n-1)\alpha}{(n-1)}\right]$ $b_n = \left(\frac{2V_{max}}{\pi}\right) \left[\frac{\sin(n+1)\alpha}{(n+1)} - \frac{\sin(n-1)\alpha}{(n-1)}\right]$ for $n \neq 1$	
load current	$i_L = \left(\frac{V_L}{R_L}\right) + \sum_{n=1}^{\infty} \sqrt{\frac{a_n^2 + b_n^2}{Z_n^2}} \cos\left(n\omega t - \tan^{-1}\left(\frac{b_n}{a_n}\right) - \phi_n\right)$	
Rms load current	$I_{LR} = \sqrt{I_L^2 + \sum_{n=1}^{\infty} I_{LnR}^2}$ with $I_{LnR} = \frac{V_{Ln}}{\sqrt{2}Z_n}$	
	By calculation	By simulation
Rms load current (A)	6.999	6.998

4.3 Controlled single-phase full-wave rectifier

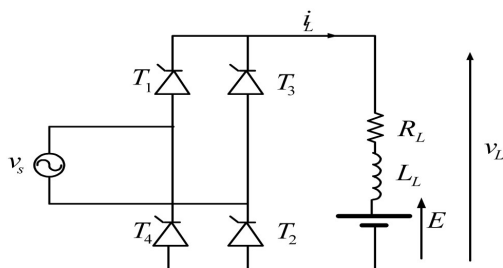


Fig. 9. Controlled single phase full-wave rectifier.

Phase voltage, and frequency	$V_{sR} = 84.85V, f_s = 60Hz$
Voltage-source type of nonlinear load (Continuous mode)	$L_L = 50mH, R_L = 80/6\Omega, \alpha = 25^\circ$
Voltage-source type of nonlinear load (Discontinuous mode)	$L_L = 20mH, R_L = 80/6\Omega, \alpha = 50^\circ$
emf	40V

Table 3. Specification parameters.

(a) Simulation results

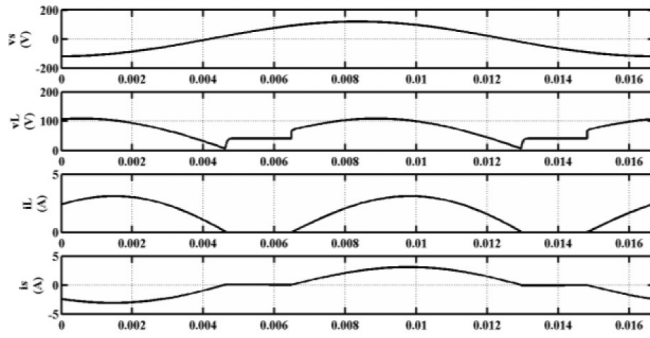


Fig. 10. Discontinuous mode $v_s(V)$, $v_L(V)$, $i_L(A)$ and $i_s(A)$.

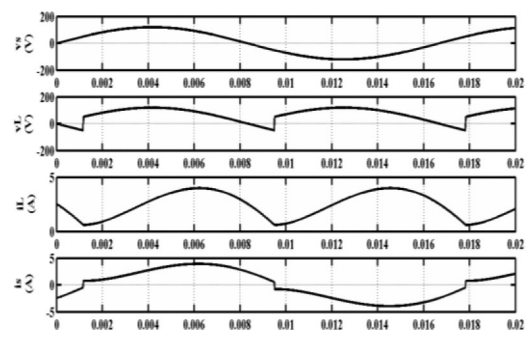


Fig. 11. Continuous mode $v_s(V)$, $v_L(V)$, $i_L(A)$ and $i_s(A)$.

(b) Experimental results

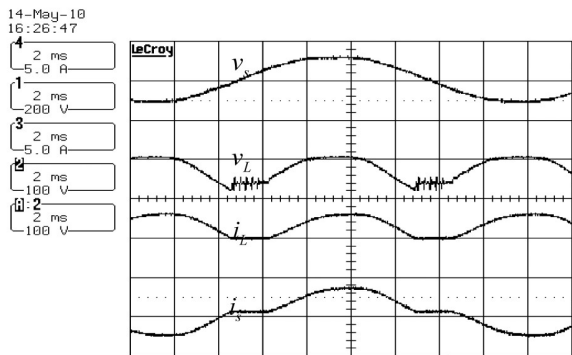


Fig. 12. Discontinuous mode $v_s(V)$, $v_L(V)$, $i_L(A)$ and $i_s(A)$.

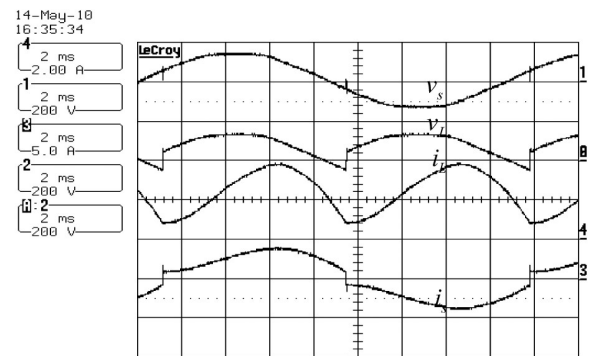


Fig. 13. Continuous mode $v_s(V)$, $v_L(V)$, $i_L(A)$ and $i_s(A)$.

Determination the curve beta versus alpha

function $F = fx5(x)$;

for $i = 1:2$;

$\alpha = [0 \quad 30 \cdot \pi / 180]$;

$Lch3 = 0.020$; $W = 2 \cdot \pi \cdot 60$; $E = 40$; $Rch3 = 12$; $Vmax = 170$; $m = E / Vmax$;

$Z = [\sqrt{Rch3^2 + (Lch3 \cdot W)^2}]$; $\Phi = [\text{atan}(Lch3 \cdot W / Rch3)]$; $\tau = [Lch3 / Rch3]$;

$F(i) = (Vmax / Z) \cdot \sin(x(i) - \Phi) - (E / Rch3) + ((E / Rch3) - (Vmax / Z)) \cdot \sin(\alpha(i) - \Phi) \cdot \exp(-x(i) / (W \cdot \tau)) \cdot \exp(\alpha(i) / (W \cdot \tau))$;

end

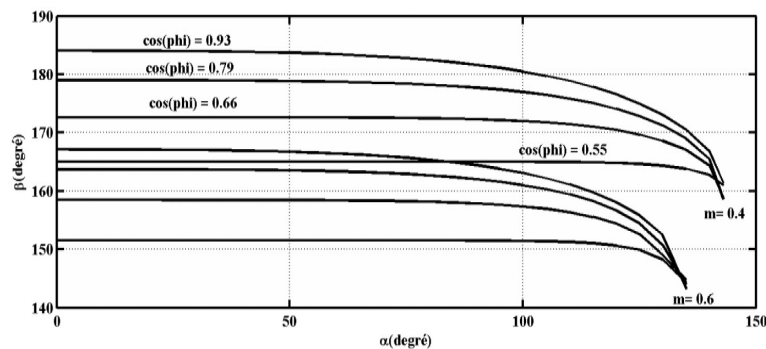


Fig. 14. Extension angle β versus firing angle α .

(a) Continuous mode

Average load voltage	Average load current	Fundamental rms line current	Rms load voltage
$V_L = \frac{1}{\pi} \int_{\alpha}^{\pi+\alpha} V_{\max} \sin \omega t \, d\omega t$ $= \frac{2V_{\max}}{\pi} \cos \alpha$	$I_L = \frac{V_L - E}{R_L}$	<p>For n inpair :</p> $a_1 = \frac{-4 * I_L * \sin(\alpha)}{\pi} \text{ and } b_1 = \frac{4 * I_L * \cos(\alpha)}{\pi}$ $I_{AR1} = \sqrt{\frac{a_1^2 + b_1^2}{2}}$	$V_{LR} = \sqrt{\frac{1}{\pi} \left[\int_{\alpha}^{\pi+\alpha} (V_{\max} \sin \omega t)^2 \, d\omega t \right]} = \frac{V_{\max}}{\sqrt{2}}$

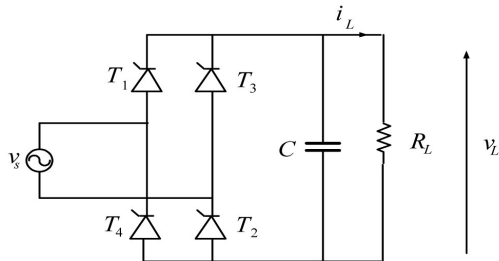
(b) Discontinuous mode

Extinction angle for $V_{\max} = 120V$	Average load voltage	Average load current	Rms load voltage
$\beta = 186.77^\circ$	$V_L = \frac{V_{\max}}{\pi} [\cos \alpha - \cos \beta + m(\pi + \alpha - \beta)]$	$I_L = \frac{V_L - E}{R_L}$	$V_{LR} = V_{\max} \sqrt{\frac{1}{\pi} \left[\frac{1}{4} (\sin 2\alpha - \sin 2\beta) + \left(\frac{1}{2} - m^2\right) (\beta - \alpha) + \pi m^2 \right]}$

	Continuous mode		Discontinuous mode	
	By calculation	By simulation	By calculation	By simulation
Load average voltage	69.23 V	69.22 V	72.09 V	71.82 V
Load average current	2.19 A	2.19 A	2.41 A	2.38 A
Rms line fundamental current	1.97 A	1.95 A	2.014 A	2.06 A
Rms load voltage	84.85 V	84.55 V	81.94 V	81.62 V

Table 4. Calculation and simulation results.

4.4 Controlled single-phase full-wave rectifier with RC load



Phase voltage, and frequency	$V_{sR} = 120V, f_s = 60Hz$
Voltage-source type of nonlinear load	$C_L = 400 \mu F, R_L = 80 \Omega, \alpha = 70^\circ$

Fig. 15. Controlled single phase full-wave rectifier with fem E.

Table 5. Specification parameters.

(a) Simulation results

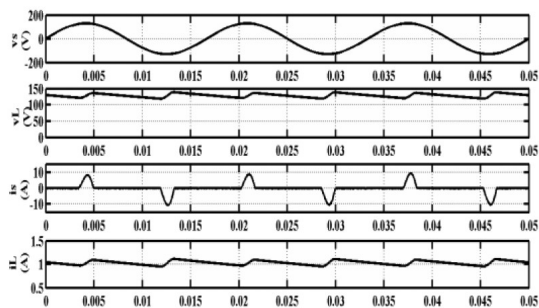


Fig. 16. Waveforms: $v_s(V), v_L(V), i_L(A)$ and $i_L(A)$.

(b) Experimental results

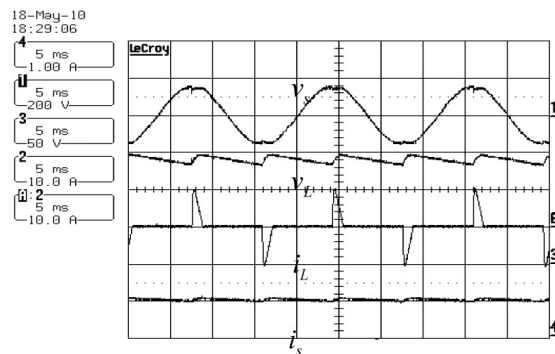


Fig. 17. Waveforms. $v_s(V), v_L(V), i_L(A)$ and $i_L(A)$.

One chooses $\Delta V = 0.25 * V_{\max}$

	By calculation	By simulation
Ripple output voltage ΔV	$\Delta V = 0.25 * V_{\max} = 42.5 V$	36 V
Load average voltage $V_L = V_{\max} - \frac{\Delta V}{2}$	148.75 V	148.8 V
Load average current $I_L = \frac{V_L}{R_L}$	1.86 A	1.87 A
Output capacitor $C = \frac{V_{\max}}{(2 * f * R_L * \Delta V)}$	416 μF	400 μF

Table 6. Calculation and simulation results.

One remarks that when the firing angle α is less than the angle α_0 shown in Fig. 18, the average load voltage is not affected, above this value the load the average voltage can be varied.

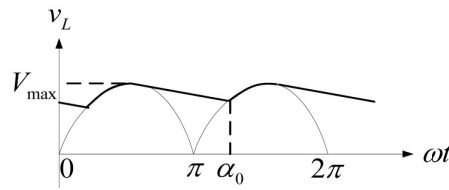
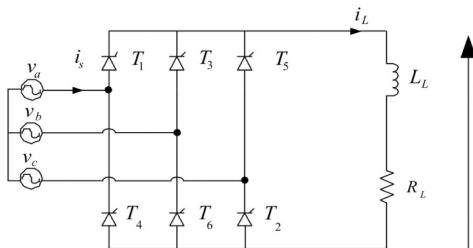


Fig. 18. Controlled single phase full-wave rectifier.

4.5 Three-phase rectifier [17]

The average value of the load current is I_L ; the rms value of the load is I_{LR} ; the rms value of the line fundamental current is I_{AR1} ; the rms value of the source current is I_{AR} ; and the rms value of the load voltage: V_{LR}

4.5.1 Three-phase controlled rectifier without freewheeling diode with RL load for $\alpha = 70^\circ$



Phase voltage, and frequency	$V_{sR} = 120V, f_s = 60Hz$
Voltage-source type of nonlinear load	$L_L = 150mH, R_L = 25 \Omega$

Fig. 19. Three-phase controlled rectifier.

Table 7. Specification parameters.

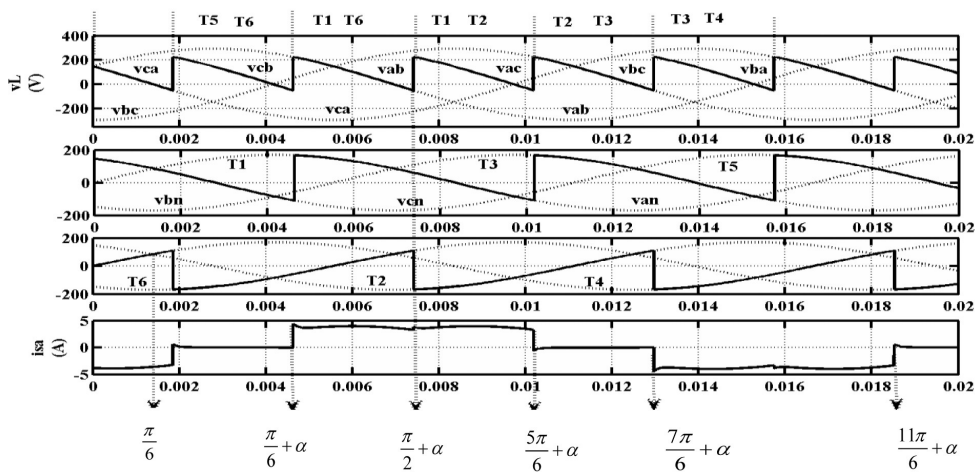


Fig. 20. Simulation waveforms for a three-phase full converter.

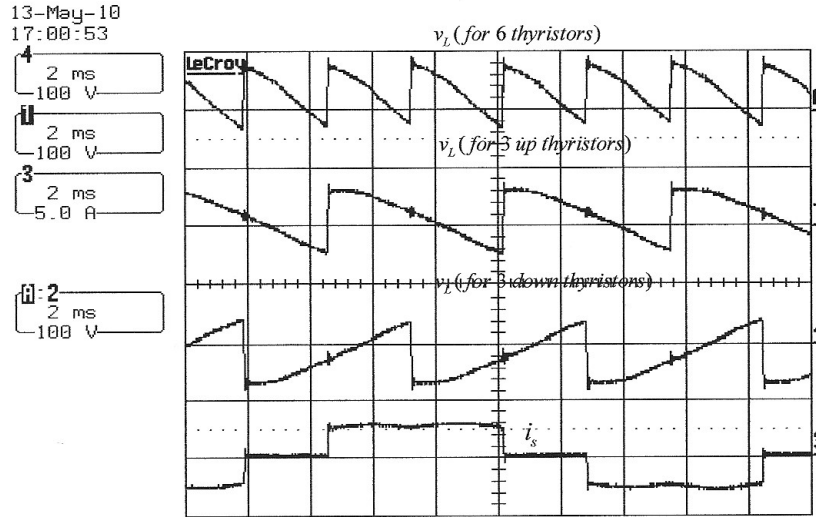


Fig. 21 Experimental waveforms for a three-phase full converter.

For proper handling to calculate correctly the currents and the voltages for a three-phase controlled rectifier it is important to identify the integration limits and the voltages set in. For this, we must address the waveforms to the terminal voltage of the load separately from the three corresponding upper thyristors (T1, T3, T5) and the three lower thyristors (T4, T6, T2). By making this difference, one can determine the output voltage. One can easily identify the sequences of operation of the rectifier and the phase voltage corresponding to each of the sections of the output voltage. For example, to calculate the average value of the voltage across the load one takes a piece of this output voltage, one marks the interval and the corresponding phase voltage. Note that the firing angle is counted from $\frac{\pi}{6}$.

$$v_{ab} = v_{an} - v_{bn} = V_{\max} \sin(\omega t) - V_{\max} \sin\left(\omega t - \frac{2\pi}{3}\right) = \sqrt{3} V_{\max} \sin\left(\omega t + \frac{\pi}{6}\right) \quad (9)$$

$$V_L = \frac{3}{\pi} \int_{\frac{\pi}{6}+\alpha}^{\frac{5\pi}{6}+\alpha} v_{ab} d\omega t = \frac{3}{\pi} \int_{\frac{\pi}{6}+\alpha}^{\frac{5\pi}{6}+\alpha} \sqrt{3} V_{\max} \sin\left(\omega t + \frac{\pi}{6}\right) d\omega t = \frac{3\sqrt{3} V_{\max}}{\pi} \left[-\cos\left(\omega t + \frac{\pi}{6}\right)\right]_{\frac{\pi}{6}+\alpha}^{\frac{5\pi}{6}+\alpha} = \frac{3\sqrt{3} V_{\max}}{\pi} \cos(\alpha) \quad (10)$$

One can also calculate the average output voltage, for example, if one changes the integration limits defined by: $\frac{\pi}{2} + \alpha$ until $\frac{5\pi}{6} + \alpha$; but in this case, one should take the phase to phase voltage v_{ac}

$$v_{ac} = v_{an} - v_{cn} = V_{\max} \sin(\omega t) - V_{\max} \sin\left(\omega t - \frac{4\pi}{3}\right) = \sqrt{3} V_{\max} \sin\left(\omega t - \frac{\pi}{6}\right) \quad (11)$$

$$V_L = \frac{3}{\pi} \int_{\frac{\pi}{2}+\alpha}^{\frac{5\pi}{6}+\alpha} v_{ac} d\omega t = \frac{3}{\pi} \int_{\frac{\pi}{2}+\alpha}^{\frac{5\pi}{6}+\alpha} \sqrt{3} V_{\max} \sin\left(\omega t - \frac{\pi}{6}\right) d\omega t = \frac{3\sqrt{3} V_{\max}}{\pi} \cos(\alpha) \quad (12)$$

	Expressions
Average output voltage and output current	$V_L = \frac{3}{\pi} \int_{\frac{\pi}{6}+\alpha}^{\frac{5\pi}{6}+\alpha} \sqrt{3} V_{\max} \sin\left(\omega t + \frac{\pi}{6}\right) d\omega t = \frac{3\sqrt{3} V_{\max}}{\pi} \cos \alpha$ and $I_L = \frac{V_L}{R_L}$
Rms fundamental input current	$a_1 = \frac{1}{\pi} \left[\int_{\frac{\pi}{6}+\alpha}^{\frac{5\pi}{6}+\alpha} I_L \cos \omega t d\omega t + \int_{\frac{11\pi}{6}+\alpha}^{\frac{11\pi}{6}+\alpha} -I_L \cos \omega t d\omega t \right] = -\frac{2\sqrt{3} I_L}{\pi} \sin \alpha$ $b_1 = \frac{1}{\pi} \left[\int_{\frac{\pi}{6}+\alpha}^{\frac{5\pi}{6}+\alpha} I_L \sin \omega t d\omega t + \int_{\frac{11\pi}{6}+\alpha}^{\frac{11\pi}{6}+\alpha} -I_L \sin \omega t d\omega t \right] = \frac{2\sqrt{3} I_L}{\pi} \cos \alpha$ and $I_{AR1} = \sqrt{\frac{a_1^2 + b_1^2}{2}} = \frac{\sqrt{6} I_L}{\pi}$
Rms input current	$I_{AR} = \sqrt{\frac{2}{T} \int_{\frac{\pi}{6}+\alpha}^{\frac{5\pi}{6}+\alpha} I_L^2 d\omega t} = \sqrt{\frac{1}{\pi} \int_{\frac{\pi}{6}+\alpha}^{\frac{5\pi}{6}+\alpha} I_L^2 d\omega t} = I_L \sqrt{\frac{2}{3}}$
Rms output voltage	$V_{LR} = \sqrt{\frac{1}{T} \int_{\frac{\pi}{6}+\alpha}^{\frac{5\pi}{6}+\alpha} \left(V_{\max} \sin\left(\omega t + \frac{\pi}{6}\right) \right)^2 d\omega t} = \sqrt{3} V_{\max} \sqrt{\frac{3}{2\pi} \left[\frac{\pi}{3} + \frac{\sqrt{3}}{2} \cos(2\alpha) \right]}$

Table 8 shows the integration limits approximately for all cases of the controlled three-phase rectifier. The integration limits are validated by calculating the input and the output variables of the three-phase controlled rectifier with a highly inductive load by theoretical calculation and by simulation using rms and average block in MATLAB.

	Three-phase controlled rectifier without freewheeling diode for $\alpha = 70^\circ$	Three-phase controlled rectifier with freewheeling diode for $\alpha = 70^\circ$	Three-phase semi controlled rectifier without freewheeling diode for $\alpha = 30^\circ$	Three-phase semi controlled rectifier with freewheeling diode for $\alpha = 70^\circ$
Parameters	Integration limits	Integration limits	Integration limits	Integration limits
$V_L (V)$	$\frac{\pi}{6} + \alpha \rightarrow \frac{\pi}{2} + \alpha$	$\frac{\pi}{6} + \alpha \rightarrow \frac{5\pi}{6}$	$\frac{\pi}{6} + \alpha \rightarrow \frac{\pi}{2}$ and $\frac{\pi}{2} \rightarrow \frac{5\pi}{6} + \alpha$	$\frac{\pi}{6} + \alpha \rightarrow \frac{7\pi}{6}$
$I_L (A)$	$\frac{\pi}{6} + \alpha \rightarrow \frac{\pi}{2} + \alpha$	$\frac{\pi}{6} + \alpha \rightarrow \frac{5\pi}{6}$	$\frac{\pi}{6} + \alpha \rightarrow \frac{\pi}{2}$ and $\frac{\pi}{2} \rightarrow \frac{5\pi}{6} + \alpha$	$\frac{\pi}{6} + \alpha \rightarrow \frac{7\pi}{6}$
$I_{ARL} (A)$	$\frac{\pi}{6} + \alpha \rightarrow \frac{5\pi}{6} + \alpha$ $\frac{7\pi}{6} + \alpha \rightarrow \frac{11\pi}{6} + \alpha$	$\frac{\pi}{6} + \alpha \rightarrow \frac{5\pi}{6}$ and $\frac{\pi}{2} + \alpha \rightarrow \frac{7\pi}{6}$ $\frac{7\pi}{6} + \alpha \rightarrow \frac{11\pi}{6}$ and $\frac{9\pi}{2} + \alpha \rightarrow \frac{13\pi}{6}$	$\frac{\pi}{6} + \alpha \rightarrow \frac{5\pi}{6} + \alpha$ $\frac{7\pi}{6} \rightarrow \frac{11\pi}{6}$	$\frac{\pi}{6} + \alpha \rightarrow \frac{7\pi}{6}$ $\frac{5\pi}{6} + \alpha \rightarrow \frac{11\pi}{6}$
$I_{AR} (A)$	$\frac{\pi}{6} + \alpha \rightarrow \frac{5\pi}{6} + \alpha$	$\frac{\pi}{6} + \alpha \rightarrow \frac{5\pi}{6}$	$\frac{\pi}{6} + \alpha \rightarrow \frac{5\pi}{6} + \alpha$	$\frac{\pi}{6} + \alpha \rightarrow \frac{7\pi}{6}$
$V_{LR} (V)$	$\frac{\pi}{6} + \alpha \rightarrow \frac{\pi}{2} + \alpha$	$\frac{\pi}{6} + \alpha \rightarrow \frac{5\pi}{6}$	$\frac{\pi}{6} + \alpha \rightarrow \frac{\pi}{2}$ and $\frac{\pi}{2} \rightarrow \frac{5\pi}{6} + \alpha$	$\frac{\pi}{6} + \alpha \rightarrow \frac{7\pi}{6}$

Table 8. Integration limits for a three-phase rectifier.

Table 9 shows a comparison between the theoretical calculation of the input and the output variables of the three-phase controlled rectifier with the measured values by simulation using rms and average block in MATLAB. One sees that there is a good correlation between the calculated values and the values given by the simulation. This validates the proposed technique for finding the appropriate integration limits for the three-phase controlled rectifier.

Parameters	Three-phase controlled rectifier without freewheeling diode for $\alpha = 70^\circ$		Three-phase controlled rectifier with freewheeling diode for $\alpha = 70^\circ$		Three-phase semi controlled rectifier without freewheeling diode for $\alpha = 30^\circ$		Three-phase semi controlled rectifier with freewheeling diode for $\alpha = 70^\circ$	
	Calculated	Simulated	Calculated	Simulated	Calculated	Simulated	Calculated	Simulated
$V_L (V)$	96.17	96.07	100.44	100.3	262.34	262.1	188.67	188.3
$I_L (A)$	3.85	3.85	4.02	4.01	10.49	10.49	7.55	7.54
$I_{ARL} (A)$	3	3	2.65	2.66	7.90	7.90	4.82	4.87
$I_{AR} (A)$	3.14	3.13	3	3.02	8.56	8.56	5.90	5.94
$V_{LR} (V)$	126.04	126.3	125.46	125.2	265.02	264.4	215.38	215.3

Table 9. Comparative table of calculated and simulation values for input and output variables for the three-phase rectifier.

4.6 Three-phase controlled rectifier with RC load for $\alpha = 45^\circ$

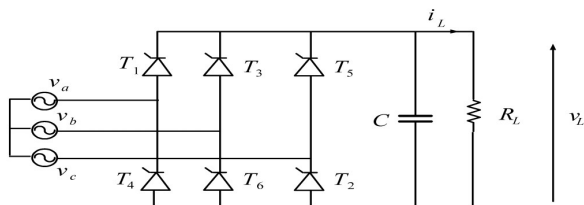


Fig. 22. Three-phase controlled rectifier.

Phase voltage, and frequency	$V_{sR} = 120V, f_s = 60Hz$
Voltage-source type of nonlinear load	$C_L = 400 \mu F, R_L = 80 \Omega$

Table 10. Specification parameters.

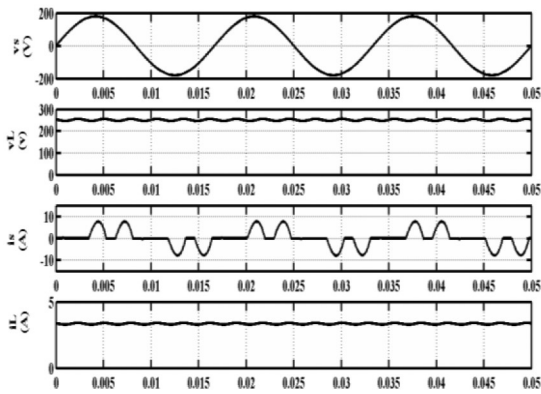


Fig. 23. Simulation: $v_s(V)$, $v_L(V)$, $i_s(A)$ and $i_L(A)$.

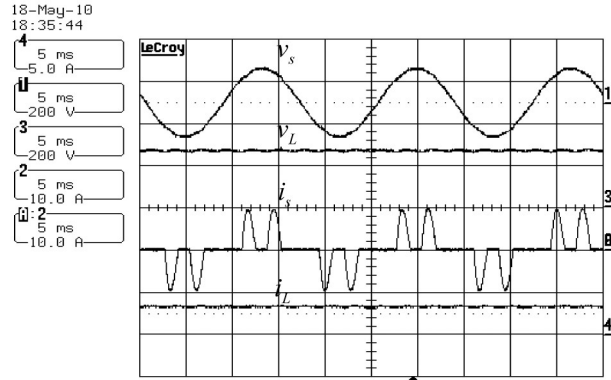


Fig. 24. Experimental: $v_s(V)$, $v_L(V)$, $i_s(A)$ and $i_L(A)$.

The ripple voltage of the load voltage is chosen as $\Delta V = 0.029 * V_{max}$ (13)

One deduces the average load voltage by $V_L = V_{max} - \frac{\Delta V}{2}$ (14)

The average load current is calculated by $I_L = \frac{V_L}{R_L}$ (15)

The loss of capacitor charge is given by $\Delta Q = C\Delta V = I_L\Delta t$ (16)

The discharging time for a diode rectifier corresponding to the angle $\frac{2\pi}{6} - \theta_c$, the filtering capacitor for a three phase diodes rectifier is calculated using the formula given by $C = \frac{I_L(\frac{2\pi}{6} - \theta_c)}{\Delta V * \omega}$ and $\theta_c = \sqrt{\frac{2\Delta V}{V_{Lmax}}} = 13.79^\circ$ [18]. For a thyristor θ_c was estimated as 39.29° .

	By calculation	By simulation
Load average voltage	290.18 V	293.1 V
Load average current	3.63 A	3.66 A
ΔV_L	8.54 V	9.4 V
Capacitor	407 μF	400 μF

Table 11. Calculation and simulation results.

5. Interactivity learning

In this process for a given circuit one can learn about interactive real-time varying elements such as load resistance and inductance and make an oscilloscope that is so interactive that one can view simulation of several waveforms associated with parameter changes of the load elements on the same diagram. All these elements are visible and handled in the same window, which explain better the phenomena encountered such as the continuous conduction mode and discontinuous conduction mode.

5.1 Modeling the variable inductance and resistance

Using the equation given below, the inductance is modeled by $v = L \frac{di}{dt} \rightarrow i = \frac{1}{L} \int v dt$ and the resistance is modeled by $v = Ri \rightarrow i = \frac{v}{R}$ as a current source.

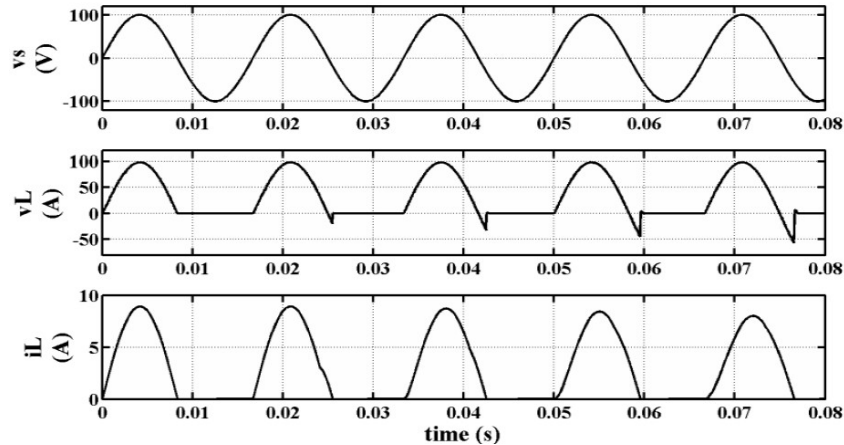


Fig. 25. Simulation results when the variable inductor is operated.

The phenomena observed in the Fig. 25 shows the effect of varying the load inductance. One sees that the negative part of the load voltage becomes greater when the inductance is increased; this can be explained by the increased stored energy in the inductance. One can see also that the slope of the load current is decreased; this explains the function of the inductance to smoothen the current and reduce the ripple current.

6. Conclusion

In this paper, methods for learning platforms for power electronics have been proposed. The methods are divided into three major parts: software simulation, software programming and, finally, theoretical calculation. The controlled rectifiers are used as an example for validation. The self-learning makes the course more attractive for the students. The proposed methods have been very positively accepted and the students have shown a great interest in the course. One can believe that our objectives of self-learning for the students have been achieved. The integration limits of different rectifiers have been identified to serve as a reference for calculations. The software programming uses the MATLAB function 'fsolve' to determine the extinction angle without using nomograms and determines the rms load current rather than the normalized (per unit) current. The calculation of the input and the output values of the three-phase controlled rectifier are presented for all cases, it shows the same values as those calculated in the simulation. From the interactive point of view, one can see all the variables varying during the simulation and the students can better understand the effects of varying parameters in a better visual manner.

References

1. N. Mohan, A. K. Jain, P. Jose and R. Ayyanar, Teaching utility applications of power electronics in a first course on power systems, *IEEE Transactions on Power Systems*, **19**(1), 2004, pp. 40–7.
2. N. Mohan, W. P. Robbins, P. Imbertson, T. M. Undeland, R.C. Panaitescu, A. K. Jain, P. Jose and T. Begalke, Restructuring of first courses in power electronics and electric drives that integrates digital control, *IEEE Transactions on Power Electronics*, **18**(1), 2003, pp. 429–37.
3. Ned Mohan, Amit Kumar Jain, Philip Jose and Rajapandian Ayyanar, Teaching utility applications of power electronics in a first course on power systems, *IEEE Transactions on Power Systems*, **19**(1), 2004, pp. 40–47.
4. F. Vasca, L. Iannelli, M. K. Camlibel and R. Frasca, A new perspective for modeling power electronics converters: complementarity framework, *IEEE Transactions on Power Electronics*, **24**(2), 2009, pp. 456–68.
5. Kenneth Wacks, The impact of home automation on power electronics, *IEEE-APEC '93 Conference*, March 1993, pp. 3–9.
6. I. Batarseh, Course and laboratory instructions in power electronics, *PESC '94 Record. 25th Annual IEEE Power Electronics Specialists Conference (Cat. No.94CH3418-1)*, 1994, Vol. 2, pp. 1359–68.
7. I. Chamas and M.A.E. Nokali, Automated PSpice simulation as an effective design tool in teaching power electronics, *IEEE Transactions on Education*, **47**(3), 2004, pp. 415–21.
8. W. Fischer and A. Lindemann, Circuit simulation in a research oriented education of power electronics, *Eleventh IEEE Workshop on Control and Modeling for Power Electronics*, 2008, pp. 5.
9. Shun-Chung Wang, Software-reconfigurable e-learning platform for power electronics courses, *IEEE Transactions on Industrial Electronics*, **55**(6), 2008, pp 2416–24.
10. N. Mohan, Teaching utility applications of power electronics in the first course on power systems, *IEEE Power Engineering Society General Meeting (IEEE Cat. No.03CH37491)*, 2003, Vol. 1, pp. 130–2.
11. E. A. McShane, M. Trivedi, K. Shenai, An improved approach to application-specific power electronics education. Curriculum development, *IEEE Transactions on Education*, **44**(3), 2001, pp. 282–8.

12. L. Max, T. Thiringer, T. Undeland and R. Karlsson, Power electronics design laboratory exercise for final-year M.Sc. students, *IEEE Transactions on Education*, **52**(4), 2009, pp. 524–31.
13. E. A. McShane, M. Trivedi, and K. Shenai,, An improved approach to application-specific power electronics education. Curriculum development, *IEEE Transactions on Education*, **44**(3), 2001, pp. 282–288.
14. William McMurry, Power Electronics in the 1990's, *IEEE-APEC'90 Conference*, March 1993, pp. 839–843.
15. I. Batarseh, Course and laboratory instructions in power electronics, *PESC '94 Record. 25th Annual IEEE Power Electronics Specialists Conference (Cat. No.94CH3418-1)*, 1994, Vol. 2, pp. 1359–68.
16. Jaeho Choi and Hyungsoo Mok, *Fourth Power Conversion Conference*, Nagoya, 2007, pp. 491–5.
17. M. H. Rashid, *Power Electronics, Circuits, Devices, and Applications*, 2nd edn, Prentice Hall, 1993.
18. J. Mignard and C. Pin, *Électronique de puissance, les redresseurs: redresseurs polyphasés à diodes, à thyristors et mixtes*, Cours et exercices corrigés, ellipses, 2010.

Auguste Ndtoungou was born in Bitam, Gabon, in 1960. He received his Ph.D. from the University of Paris XI, France, in 1996. From 1997, he was a Professor in the École Polytechnique de Masuku in Gabon. Currently he is in the Department of Electrical Engineering, École de Technologie Supérieure, Montréal, Canada. His research interests include power electronics, power quality and renewable energy.

Abdelhamid Hamadi was born at Bejaia, Algeria. He received his Bachelor of Engineering from University of Polytechnics of Algier in 1987 and Master of Technology degrees in Electrical Engineering from École de Technologie Supérieure in Montréal, Québec in 2004. Presently he is working for his Ph.D. in the Department of Electrical Engineering, École de Technologie Supérieure, Montréal, Canada. His research interests include the Application of Power Electronics in Distribution Systems, Power Quality Analysis, Active Power Filters, Hybrid power Filters, series hybrid filter and Passive Filters.

Kamal Al-Haddad was born in Beirut, Lebanon, in 1954. He received his B.Sc.A. and M.Sc.A. degrees from the university of Québec à Trois-Rivières, Trois-Rivières, QC, Canada, in 1982 and 1984, respectively, and his Ph.D. from the Institut National Polytechnique, Toulouse, France, in 1988.

From June 1987 to June 1990 he was a Professor with the Engineering Department, Université du Québec à Trois Rivières. Since June 1990, he has been a Professor with the Electrical Engineering Department, École de Technologie Supérieure (ETS), Montreal, QC, where he has been the holder of the Canada Research Chair in Electric Energy Conversion and Power Electronics since 2002. He has supervised more than 60 M.Sc.A. and Ph.D. students working in the field of power electronics. He was the Director of graduate study programs at ETS from 1992 to 2003. He is a Consultant and has established very solid links with many Canadian industries working in the field of power electronics, electric transportation, aeronautics and telecommunications. He is the Chief of the ETS-Bombardier transportation North America Division, a joint industrial research laboratory on electric traction system and power electronics. He is the coauthor of the Power System Blockset software of MATLAB. His fields of interests include high-efficient static power converters, harmonics and reactive power control using hybrid filters, and switch-mode and resonant converters, including the modeling, control, and development of prototypes for various industrial applications in electric traction, power supply for drives, telecommunication, etc.

Professor Al-Haddad is a Life Member of the Circle of Excellence of the University of Quebec and received the Outstanding Researcher Award from ETS in 2000. He is very active in the industrial Electronics Society where he is an V.P. Technical activities, AdCom Member and serves as an Associate editor for *IEEE Transactions on Industrial Electronics*.